



ELSEVIER

Contents lists available at ScienceDirect

Journal of Differential Equations

www.elsevier.com/locate/jde



# Neural spike renormalization. Part I – Universal number 1

Bo Deng

Department of Mathematics, University of Nebraska-Lincoln, Lincoln, NE 68588, United States

## ARTICLE INFO

### Article history:

Received 21 July 2010

Available online xxxx

### Keywords:

Circuit models of neurons

Poincaré return maps

Feigenbaum constant

Period-doubling bifurcation

Isospike bifurcation

Renormalization universality

## ABSTRACT

For a class of circuit models for neurons, it has been shown that the transmembrane electrical potentials in spike bursts have an inverse correlation with the intra-cellular energy conversion: the fewer spikes per burst the more energetic each spike is. Here we demonstrate that as the per-spike energy goes down to zero, a universal constant to the bifurcation of spike-bursts emerges in a similar way as Feigenbaum's constant does to the period-doubling bifurcation to chaos generation, and the new universal constant is the first natural number 1.

© 2010 Elsevier Inc. All rights reserved.

## 1. Introduction

It is often the case that certain intrinsic property of a physical process is hidden, and it requires some iterative operation to grind it out. Such iterative operations usually go by the name of renormalization in physics. Mitchell Feigenbaum discovered in the late 70s [20,21] a renormalization from his study of the logistic map,  $x_{n+1} = Q_\lambda(x_n) = \lambda x_n(1 - x_n)$ , which led to an important understanding on a universal passage from order to chaos in nature.

On the surface of it, the period-doubling bifurcation points  $\lambda_k$  converge to a limit  $\lambda_\infty$  at an exponential rate  $|\lambda_k - \lambda_\infty| \sim 1/\delta^k$  for which  $\delta = 4.669201\dots$  is known as the *Feigenbaum constant*. But at a deeper fundamental level, the sequence is associated with a renormalizing operator in a functional space of renormalizable unimodal maps to which the logistic maps also belong, and the Feigenbaum constant is the only expanding eigenvalue of the renormalizing operator at a fixed point. More specifically, the fixed point has a one-dimensional unstable manifold with  $\delta$  being its expanding eigenvalue and a co-dimension-one stable manifold containing  $Q_{\lambda_\infty}$  at which chaos first appears as  $\lambda$  passes through  $\lambda_\infty$  from below (see also [22,1,2]). The dynamical view of the logistic family  $\{Q_\lambda: \lambda \in [0, 4]\}$  in this renormalization space is that of a curve transversal to the stable manifold at  $Q_{\lambda_\infty}$  and the iterations of the family under the renormalizing operator approach the unstable manifold – a clas-

E-mail address: [bdeng1@math.unl.edu](mailto:bdeng1@math.unl.edu).

0022-0396/\$ – see front matter © 2010 Elsevier Inc. All rights reserved.

doi:10.1016/j.jde.2010.10.002

Please cite this article in press as: B. Deng, Neural spike renormalization. Part I – Universal number 1, J. Differential Equations (2010), doi:10.1016/j.jde.2010.10.002

sical view of the inclination lemma [23,4,5,3] at hyperbolic fixed points of all dynamical systems. In this setting of renormalization, the limit that  $\lim_{k \rightarrow \infty} \frac{\lambda_n - \lambda_{n+1}}{\lambda_{n+1} - \lambda_{n+2}} = \delta$  is a quantitative consequence to the inclination lemma. For all physical processes which go through the route of period-doubling to chaos, they are expected to represent different families in the renormalization space, both qualitatively similar to the logistic family and quantitatively the same at the converging limit to the unstable manifold of the fixed point. That is, their passages to chaos will always produce the same Feigenbaum constant, and it is in this sense that the Feigenbaum constant is universal to period-doubling cascade to chaos.

In this paper we will consider a different type of bifurcation and a new renormalization universality but otherwise completely parallel to Feigenbaum's renormalizing paradigm outlined above. The context from which the new problem arises is about the generation of spiking bursts used as alphabet for neural communication, computation, and memory [15–18].

More specifically, we will show how the generation of transient electrical bursts of spikes across neuron's excitable membranes can be qualitatively approximated by a simplistic but prototypical map,  $\psi_\mu : [0, 1] \mapsto [0, 1]$  where  $\psi_\mu(x) = x + \mu$  if  $0 \leq x < 1 - \mu$  and  $\psi_\mu(x) = 0$  if  $1 - \mu \leq x \leq 1$  for which  $0 < \mu < 1$  is a parameter proportional to the total absolute current through neuron's ion pumps that in turn is related to its intra-cellular biochemical energy conversion [17].

In this setting, the right interval  $J_1 = [1 - \mu, 1]$  corresponds to the cell's refractory phase when transmembrane spikes are absent and the left interval  $J_0 = [0, 1 - \mu]$  corresponds to the spiking phase. Instead of periodic bifurcation we will consider the so-called *isospiking* bifurcation points  $\mu_n$  so that for  $\mu_{n+1} < \mu < \mu_n$  and for any initial point  $x_0$  from the refractory/silent phase  $J_1$  the orbit  $\{x_k : x_k = \psi_\mu^k(x_0), k \geq 0\}$  will have exactly the first  $n$  iterates  $x_1, x_2, \dots, x_n$  in the active phase  $J_0$  before the  $(n + 1)$ th iterate falls back to  $J_1$ . In other words, the refractory points  $x_0, x_{n+1}$  represent the before-and-after silent phases of an electrical burst and the transient iterates  $x_1, \dots, x_n$  represent the spikes of the burst with each  $x_k$  corresponding uniquely to one spike. For the prototypical family  $\psi_\mu$ , it is straightforward to derive the isospiking bifurcation points as  $\mu_n = 1/n$  from the bifurcation equation  $x_n = (n - 1)\mu = 1 - \mu$  where  $1 - \mu$  is the discontinuity point separating the refractory and the spiking phases. Rather than exponential,  $\mu_n$  converges to its limit  $\mu_\infty = 0$  at an arithmetic rate in the order of  $1/n$ , and the quotients of adjacent isospiking intervals,  $\frac{\mu_n - \mu_{n+1}}{\mu_{n+1} - \mu_{n+2}} = 1 + \frac{2}{n}$ , converge to 1 at the same rate as  $1/n$ .

However, the purpose of this paper is to demonstrate that one-dimensional maps which more accurately approximate the generation of bursting spikes than the simplistic family  $\psi_\mu$  exhibit the same quantitative properties for the isospiking bifurcations as the prototypical kind does and it can be understood by a unifying renormalization parallel to Feigenbaum's but unique in two aspects: the neural spike renormalization has a non-hyperbolic fixed point with a one-dimensional center-unstable manifold; and the first natural number 1 is the weakly-expanding eigenvalue along the manifold. Namely the first natural number 1 is a universal constant new in the sense of renormalization but old in every conceivable definition for what is meant known. What the Feigenbaum constant to chaos generation is what the first natural number 1 to neural spike generation.

The paper is outlined as follows. In Section 2 we will illustrate how maps such as  $\psi_\mu$  can be constructed from the dynamics of a class of circuit models for neurons. The idea of isospiking bifurcation will be introduced in Section 3. In Section 4 we will introduce the neural spike renormalization group and prove the main result, Theorem of Universal Number 1. As a sequel to this paper, we will show in [19] that, unlike the monolithic saddle structure of Feigenbaum's renormalization, the neural spike renormalization is extremely dynamical: the center-stable manifold of its fixed point contains a chaotic region into which all finitely dimensional systems can be conjugately embedded not just once but infinitely many times and all are connected to each other by a dense orbit.

## 2. Circuit models of neurons and spike return map

We will use a prototypical circuit model of neurons to motivate the general approach and result of the paper. The model is referred to as a  $pK^+sNa^+$  model because of the following assumptions which it incorporates. (1) It assumes that the electrical and the diffusive channels for the potassium ion  $K^+$  goes through the neuron membrane in parallel (represented by the letter string 'pK<sup>+</sup>' in the

model's name) that usually results in an  $N$ -shaped nonlinearity for the  $IV$ -characteristic curve of the combined parallel channel. (2) It assumes that the electrical and the diffusive channels for the sodium ion  $\text{Na}^+$  go through the neuron membrane in series (represented by the letter string 'sNa<sup>+</sup>' instead) that usually results in an  $S$ -shaped nonlinearity for the  $IV$ -characteristic curve of the combined serial channel. These channels are the passive kind determined by Ohm's law of electromagnetism and elemental diffusion. (3) It assumes that there is a joint ion pump that transports  $\text{Na}^+$  outside the cell and  $\text{K}^+$  inside (represented by the subscript '+' and '-' signs of the model taxonomy) and that the ion pump characteristic is  $A'/A \sim V$  with  $A$  representing the pump current of a given ion species and  $V$  the voltage across the pump. (4) It assumes that the passive electrical and diffusive channels have an extra-cellular resting potential for  $\text{Na}^+$  and an intra-cellular resting potential for  $\text{K}^+$  consisting with their respective transporting direction of the ion pump. In contrast, the ion pump channel is the active kind which requires the intra-cellular energy conversion by the ATPase process to operate. (5) The last assumption is to take the bilipid cell membrane to be a linear capacitor. The corresponding circuit model in differential equations is

$$\begin{cases} CV'_C = -[I_{\text{Na}} + f_K(V_C - \bar{E}_K) + I_{\text{Na pump}} - I_{\text{K pump}} - I_{\text{ext}}], \\ I'_{\text{Na pump}} = \lambda I_{\text{Na pump}} [V_C - \gamma(I_{\text{Na pump}} - I_{\text{K pump}})], \\ I'_{\text{K pump}} = \lambda I_{\text{K pump}} [-V_C + \gamma(I_{\text{Na pump}} - I_{\text{K pump}})], \\ \epsilon I'_{\text{Na}} = V_C - \bar{E}_{\text{Na}} - h_{\text{Na}}(I_{\text{Na}}). \end{cases} \tag{1}$$

Here,  $V_C$ ,  $I_{\text{Na pump}}$ ,  $I_{\text{K pump}}$ ,  $I_{\text{Na}}$  are, respectively, the transmembrane voltage, the sodium ion pump current, the potassium ion pump current, and the sodium ion current through its serial electrical and diffusive channels.  $I_{\text{ext}}$  is any forcing current external to the circuit if any. The potassium ion current through its parallel electrical and diffusive channels is given by the  $IV$ -characteristic  $I_K = f_K(V_C - \bar{E}_K)$ . The ideal  $S$ -shaped  $IV$ -characteristic is represented by  $V_C - \bar{E}_{\text{Na}} - h_{\text{Na}}(I_{\text{Na}}) = 0$  which is approximated by the singular perturbation with small  $0 < \epsilon \ll 1$  for the  $I_{\text{Na}}$ -equation. We refer to [15] for a detailed derivation of this model as well as its generalizations to other types of circuit models including an analogous  $\text{pNa}^+ \text{sK}^+$  type model, and models comprised of mixed ion species to give the respective serial and parallel  $IV$ -characteristics.

The  $\text{pK}^+ \text{sNa}^+$  model has an equivalent form by transforming the ion pump currents into their net current  $I_{\text{pump}} = I_{\text{Na pump}} - I_{\text{K pump}}$  and their absolute current  $I_S = I_{\text{Na pump}} + I_{\text{K pump}}$  (equivalently  $I_{\text{Na pump}} = \frac{1}{2}(I_S + I_{\text{pump}})$ ,  $I_{\text{K pump}} = \frac{1}{2}(I_S - I_{\text{pump}})$ ). With this change of variables the model is transformed into

$$\begin{cases} CV'_C = -[I_{\text{Na}} + f_K(V_C - \bar{E}_K) + I_{\text{pump}} - I_{\text{ext}}], \\ I'_{\text{pump}} = \lambda I_S [V_C - \gamma I_{\text{pump}}], \\ I'_S = \lambda I_{\text{pump}} [V_C - \gamma I_{\text{pump}}], \\ \epsilon I'_{\text{Na}} = V_C - \bar{E}_{\text{Na}} - h_{\text{Na}}(I_{\text{Na}}). \end{cases} \tag{2}$$

It is useful to note that the nontrivial part ( $I_{\text{pump}} \neq 0$ ) of  $I_S$ 's nullcline is exactly the same as  $I_{\text{pump}}$ 's nullcline,  $V_C = \gamma I_{\text{pump}}$ , with  $I_S > 0$  always; and that all the nullcline hypersurfaces are independent of  $I_S$ . This helps tremendously to visualize the 4-dimensional system in the 3-dimensional phase space of variables  $V_C$ ,  $I_{\text{pump}}$ ,  $I_{\text{Na}}$  as shown in Fig. 1(a). In other words, for every value  $I_S > 0$ , its three-dimensional slice in variables  $V_C$ ,  $I_{\text{pump}}$ ,  $I_{\text{Na}}$  in the full 4-dimensional phase space is exactly the same as depicted by the portrait. It shows that the full dynamics is essentially determined by the nullcline structures of the three variables. Moreover, the  $I_S$ -equation is rather simple and it can be solved explicitly as  $I_S(t) = I_S(0) + \int_0^t \lambda I_{\text{pump}}(\tau) [V_C(\tau) - \gamma I_{\text{pump}}(\tau)] d\tau$ . More importantly, as shown in Fig. 1(c), the absolute ion pump current  $I_S(t)$  seems to change very little during any episode of spike-burst, which amounts to what is referred to as the phenomenon of metastability and plasticity [16]. As an approximation, we can fix  $I_S(t)$  to be a constant for each spike-burst and reduce

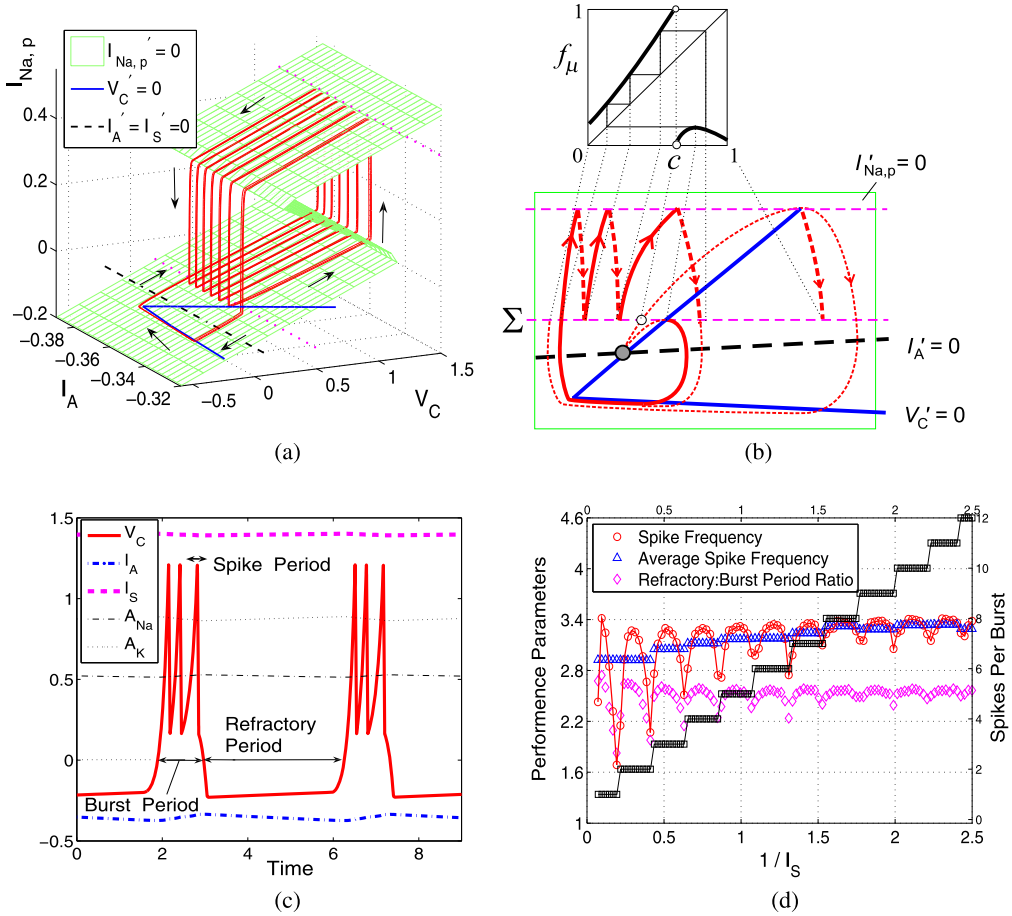


**Fig. 1.** (a) A spike-burst of 7 spikes for Eq. (2). (b) The construction of a Poincaré return map  $f_\mu$ . (c) Terminology legend for spike-bursts. (d) An isopiking bifurcation plot of the circuit model with the spike frequency defined to be the spike number divided by the burst period.

the 4-dimensional system equation (2) to this 3-dimensional system in variables  $V_C$ ,  $I_{pump}$ ,  $I_{Na}$  as follows

$$\begin{cases} CV'_C = -[I_{Na} + f_K(V_C - \bar{E}_K) + I_{pump} - I_{ext}], \\ I'_{pump} = \lambda I_S[V_C - \gamma I_{pump}], \\ \epsilon I'_{Na} = V_C - \bar{E}_{Na} - h_{Na}(I_{Na}). \end{cases} \quad (3)$$

This means both the spike-burst dynamics of the full system (2) and its lower-dimensional approximation (3) are captured by the same nullcline structure of Fig. 1(a).

Saving the explicit forms for the  $S$  and  $N$  nonlinearities for the passive  $IV$ -characteristics as well as the choices of parameter values to the cited references, one can nonetheless see clearly in Fig. 1(a) how spike-bursts are generated. It shows that the spikes are produced by the  $S$ -nonlinearity of the  $I_{Na}$ -nullcline  $V_C - \bar{E}_{Na} - h_{Na}(I_{Na}) = 0$  whereas the onset of burst is produced by the  $N$ -nonlinearity of  $K^+$ 's  $IV$ -characteristic setting on the lower branch of the  $S$ -surface. The  $I_{pump}$ -nullcline simply gates the system either into the silent/refractory phase when  $I_{pump}(t)$  decreases or into the spiking phase where the train of spikes moves in the increasing direction of  $I_{pump}$ . Precise analysis by singular

perturbations for various spike-burst generations can also be found in [6,7,9–14] for tritrophic food chain models.

It should be noted that most spike-bursts for Eqs. (1), (2) are only transient states rather than asymptotic ones [16]. With the assumption that these so-called metastable and plastic spike-bursts with varying spike numbers per-burst form an information coding alphabet, it was shown in [17] that a communication system can be constructed using one neuron circuit as an encoder and another neuron circuit, the same or different type, as a decoder, which suggests the existence of some universality for permitting such a communication system between different neurons.

Such inherent universality is suggested by the bifurcation diagram of Fig. 1(d). The diagram is generated by the following steps. We first pick an arbitrary point from the silent phase in variables  $V_C$ ,  $I_{\text{pump}}$ ,  $I_{\text{Na}}$  and fix a set of parameters which generate spike-bursts. Then for each value  $I_S$  from a set of discrete points between an interval we numerically solve the system (1) (or (2)) for the length of the subsequent one burst of spikes. The period of burst and the number of spikes are calculated according to the definitions depicted in Fig. 1(c) and then plotted in Fig. 1(d). For example, for  $I_S = 1$ , the plot shows two things: there are 5 spikes for the transient burst and the spike frequency is about 3.3 spike per unit time which interchangeably translates to  $5/3.3$  time units for the 5-spike burst period. The diagram suggests two properties. First, as  $I_S \rightarrow 0$  (or  $1/I_S \rightarrow \infty$  as actually shown), the spike frequency levels off, tending to a constant. Second, if we let  $I_S = b_n$  denote the points at which a burst of  $n$  spikes poises to change to a burst of  $n + 1$  spikes (e.g.  $I_S = 2$  would be approximately the  $b_9$  point), then the sequence  $1/b_n$  is proportional to the spike number  $n$ , i.e.

$$\frac{1}{b_n} \sim n \quad \text{equivalently} \quad b_n \sim \frac{1}{n}.$$

The underlying implication of [17] is that because different neurons would possess this universal property, their respective bifurcation points  $b_n$  can be perfectly aligned against each other by scaling just one parameter which is thought to proportionate individual neuron's intra-cellular APTass energy conversion; and as a result the alignment will allow the spike-burst information to transmit from one neuron to another. More importantly, since the absolute ion pump current  $I_S$  is thought to correlate the intra-cellular APTass energy conversion, such spike-burst communication can be achieved by only adjusting the receiving cell's biochemical energy conversion rate.

The purpose of this paper is to give a mathematical treatment to the bifurcation diagram Fig. 1(d) and its implied universality. We will do so by studying how spike-bursts are generated by Poincaré return maps. Fig. 1(b) gives an illustration to the construction of such a map  $f_\mu$ , and detailed constructions and analyses for various return maps of similar and different types can also be found in [9–14] for ecological models cited above. We begin here by looking at the phase space Fig. 1(a) from a point above the  $S$ -surface and straight down the  $I_{\text{Na}}$ -axis. Another way to state this is to look at the projections of the nullclines and the orbits on the  $I_{\text{pump}} V_C$ -plane, and then the view will be what we see in Fig. 1(b).

More specifically, the horizontal dashed lines represent the lower knee edge and the upper knee edge of the  $S$ -surface. The bold dash curves between the line edges represent orbits on the upper branch of the  $S$ -surface ending on the lower knee  $\Sigma$  at which all orbits plunge to the lower branch of the  $S$ -surface. On the lower branch, the reduced two-dimensional phase portrait is a bit more interesting, represented by both the bold solid curves and dotted curves. For the nullcline configuration shown, the 2-dimensional phase portrait is essentially a spiralling source. That is, all orbits (except for the unstable equilibrium point) on the lower branch will eventually hit the lower knee edge of the  $S$ -surface, and then jump upward to the upper branch as shown in Fig. 1(a). Ideally, the plunges and the jumps between the two branches of the surface are instantaneous, but for practical purposes they are approximated by fast orbits from the singularly perturbed  $I_{\text{Na}}$ -equation for small  $\epsilon$ . In any case, the so-called singular orbital description given above and the perturbed case for small  $\epsilon$  approximate each other well, one can be used as an approximation of the other.

In sum, the spike-bursts result from the interplay between the reduced 2-dimensional dynamics on the upper and lower branches of the  $S$ -surface. If we track the coming and going of each point from the line  $\Sigma$  following the concatenation of singular orbits from the two branches, we see how

a 1-dimensional return map emerges from the sketch. For example, point  $c$  is a discontinuity point of the map  $f_\mu$ : to the left of it, the map is monotonically increasing, driven by the progression of spikes, but to the right it is unimodal because of the resetting effect of the refractory dynamics. The particular portrait shows the iterates of the map when the initial point starts from the maximal point of the right sub-interval  $[c, 1]$ , and each subsequent iterate in the left interval corresponds to one spike during the burst. In other words, the left interval codes the active, spiking phase of the neuron circuit, the right interval codes the silent phase, and the point  $c$  for spike termination. The correspondence between the map and the absolute ion pump current  $I_S$  is that the smaller  $I_S$  is the more spikes per burst there are (Fig. 1(d)) and the closer the graph of the map is to the diagonal line as a result, which is coded by the parameter  $\mu$  in proportional to  $I_S$ :  $\mu \sim I_S$ .

Quantitatively, the graph on the right interval is rather flat because all the orbits rising within are pulled exponentially to the bottom branch of the  $V_C$ -nullcline before turning around at the leftward-pointing turning point of the  $V_C$ -nullcline. That is,  $\max_{x \in [c, 1]} f_\mu(x) \sim e^{-1/\mu}$  (cf. [8]). In contrast, because of the absence of such a pull by pseudo-equilibria, the first progression of spikes has the order of  $\mu$ , namely,  $f_\mu(0) \sim \mu$ , leading to the following property that will be assumed later for the bifurcation of spikes,

$$\max_{x \in [c, 1]} f_\mu(x) < f_\mu(0).$$

The prototypical example introduced in the previous section,  $\psi_\mu(x) = (x + \mu)H(1 - \mu - x)$  with  $H(x)$  being the Heaviside function ( $H(x) = 0$  if  $x \leq 0$  and  $H(x) = 1$  if  $x > 0$ ), is a further simplification of such spike return maps by completely flattening its right interval graph as an approximation to its exponentially flatness in general.

### 3. Isospiking bifurcations

In this section we now give a precise definition for the class of 1-dimensional spike maps and the definition of isospiking bifurcations for the maps.

**Definition 1.**  $Y$  is the set of mappings  $g: [0, 1] \rightarrow [0, 1]$  satisfying the following conditions (a)–(d):

- (a) For each  $g \in Y$  there is a constant  $c_0^g \in (0, 1]$  such that  $g$  is continuous everywhere except at  $x = c_0^g$ .
- (b)  $g$  is strictly increasing in interval  $[0, c_0^g]$ .
- (c)  $g(x) \geq x$  for  $x \in [0, c_0^g]$ .
- (d)  $\lim_{x \rightarrow (c_0^g)^+} g(x)$  exists and  $g(x) \leq g(0)$  for  $c_0^g \leq x \leq 1$ .

$Y$  is equipped with the  $L^1$  norm,  $\|g\| = \int_0^1 |g(x)| dx$ , i.e.  $Y$  is a subset of the  $L^1[0, 1]$  Banach space. Such a map is referred to as a *spike map*.

**Remark.** The value of  $g$  at the point of discontinuity  $c_0^g$  is not important because of the  $L^1$ -topology. For convenience one can set  $g(c) = g(c^-) = \lim_{x \rightarrow c^-} g(x)$  with  $c = c_0^g$  since the left limit always exists by the monotonicity of  $g$  in the left interval  $[0, c_0^g]$ . Because of this reason, any continuous increasing function  $g$  in  $[0, 1]$  with  $g(x) \geq x$  belongs to  $Y$  since one can consider  $c_0^g = 1$ . In particular, the identity function  $y = id(x) = x$  is in  $Y$ . We also note that by the  $L^1$  norm,  $\|g - h\|$  simply measures the *average distance*  $|g(x) - h(x)|$  over interval  $[0, 1]$  between the two curves  $y = g(x)$ ,  $y = h(x)$ . If there is no confusion we will use  $c_0$  to denote the point of discontinuity  $c_0^g$ .

**Definition 2.** A map  $g \in Y$  is said to be *isospiking* if there is a natural number  $n \geq 1$  so that for every point  $x^0$  from  $(c_0, 1]$  (the silent or refractory interval) the subsequent  $n$  iterates  $x^k = g^k(x^0)$ ,  $1 \leq k \leq n$ , are in  $[0, c_0]$  (the active or spiking interval) but the  $(n + 1)$ st iterate  $x^{n+1}$  falls back to

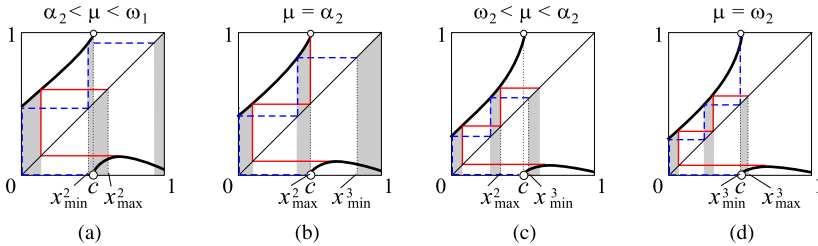


**Fig. 2.** (a) A spike map  $g_\mu$  of a family is not isospiking because the critical point splits an iteration of the right interval. The iterative intervals correspond with the shaded bars. The family is between the transition between 1-spike bursts and 2-spike bursts. (b, c, d) The family is all isospiking with (b) corresponding to the beginning and (d) the ending of the isospiking-2 parameter interval.

$(c_0, 1]$ . The number  $n$  is referred to as the *isospike number* or *spike number* for short. A map is said to be *not isospiking* if there are points from its right interval that give rise to different numbers of subsequent iterates in its left interval.

The result below shows that whether or not a map is isospiking can be determined by following the iterates of the minimal and maximal points of the refractory interval.

**Proposition 1.** Let  $x_{\min}^0, x_{\max}^0$  be the minimal and maximal points from  $[c_0, 1]$ , i.e.  $g(x_{\min}^0) = \min_{[c_0, 1]} g(x)$ ,  $g(x_{\max}^0) = \max_{[c_0, 1]} g(x)$ , and  $x_{\min}^k = g^k(x_{\min}^0), x_{\max}^k = g^k(x_{\max}^0)$ . Assume  $g(x) < g(0)$  for  $x \in [c_0, 1]$ . Then  $g$  is isospiking if and only if there is a natural number  $n$  so that

$$x_{\max}^n \leq c_0 < x_{\min}^{n+1}. \tag{4}$$

And  $g$  is not isospiking if and only if for some natural number  $n$  we have  $x_{\min}^n \leq c_0 < x_{\max}^n$ .

**Proof.** Because of the definition and the assumption, we must first have  $x_{\min}^1 \leq x_{\max}^1 < g(0)$  and  $x_{\min}^1 \leq x^k \leq x_{\max}^1 < g(0)$  for all  $x^k \in [0, c]$  with  $c = c_0$  here and below. Since  $g$  is monotonically increasing in the spiking interval the ordering  $x_{\min}^k \leq x^k \leq x_{\max}^k$  must be preserved as long as these iterates are in  $[0, c]$ . Because of  $g(x) < g(0), x \in [c, 1]$ , the first iterative interval of  $[c, 1]$  must lie inside  $[0, g(0)]$ :  $[x_{\min}^1, x_{\max}^1] \subset [0, g(0)]$ . Let  $n$  be the first iterate so that  $g^{n-1}(0) \leq c < g^n(0)$ . Because of the monotonicity of  $g$  in the spiking interval, the  $n$ th iterative interval  $[x_{\min}^n, x_{\max}^n]$  and the critical point  $c$  all lie in  $[g^{n-1}(0), g^n(0)]$ . We now see that  $g$  is isospiking of either spike number  $n$  if  $c$  lies above the  $n$ th iterative interval  $[x_{\min}^n, x_{\max}^n]$  with  $g^{n-1}(0) \leq x_{\min}^n \leq x_{\max}^n \leq c < g^n(0) \leq x_{\min}^{n+1}$  or of spike number  $n - 1$  if  $c$  lies strictly below the interval  $[x_{\min}^n, x_{\max}^n]$  with  $g^{n-1}(0) \leq c < x_{\min}^n \leq x_{\max}^n < g^n(0)$ . In the last case,  $x_{\max}^{n-1} < g^{n-1}(0) \leq c < x_{\min}^n$ , the condition (4) with  $n - 1$  for  $n$ . Whenever  $c$  splits the  $n$ th iterative interval in the sense that  $x_{\min}^n \leq c < x_{\max}^n$ ,  $g$  is not isospiking because  $x_{\min}^0$  generates  $n$  spikes but  $x_{\max}^0$  generates  $n - 1$  spikes.  $\square$

**Definition 3.** Let  $g_\mu$  be a continuous 1-parameter family of spike-renormalizable maps satisfying the condition of Proposition 1. A parameter value  $\mu = \alpha_n$  is called the *n*th *alpha isospiking bifurcation point* if  $x_{\max}^n = g_{\alpha_n}^n(x_{\max}^0) = c_0^n$ . A parameter value  $\mu = \omega_n$  is called the *n*th *omega isospiking bifurcation point* if  $x_{\min}^{n+1} = g_{\omega_n}^{n+1}(x_{\min}^0) = c_0^n$ . The interval  $\omega_n \leq \mu \leq \alpha_n$  (or  $\alpha_n \leq \mu \leq \omega_n$ ) is referred to as the *n*th *isospiking interval*.

Fig. 2 gives an illustration for the isospiking bifurcations from isospike number 1 to 3. The  $\alpha$ -bifurcation points can be considered as the beginning of isospiking parameter intervals whereas the  $\omega$ -points the ending of such intervals. For special family of spike maps  $\psi_\mu$  one can check that  $\alpha_n = \omega_{n-1} = 1/n$ .

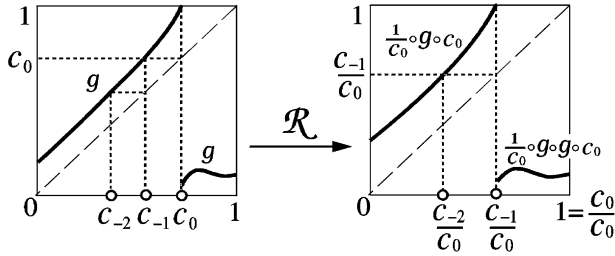


Fig. 3. A geometric illustration for  $\mathcal{R}$ .

4. Renormalization universality

We now introduce the renormalization operator  $\mathcal{R}$  and prove later the universality of the first natural number for the isospiking bifurcations of spike maps.

**Definition 4.** Let  $D = \{g \in Y : \exists c_{-1} \in (0, c_0) \text{ such that } g(c_{-1}) = c_0\}$ . The renormalizing operator  $\mathcal{R} : D \rightarrow Y$  is defined as follows

$$g \in D \rightarrow \mathcal{R}[g](x) = \begin{cases} \frac{1}{c_0} g(c_0 x), & 0 \leq x < \frac{c_{-1}}{c_0}, \\ \frac{1}{c_0} g \circ g(c_0 x), & \frac{c_{-1}}{c_0} \leq x \leq 1. \end{cases} \tag{5}$$

A spike map from  $D$  is referred to as renormalizable.

**Remark.** Though it looks like a doubling map of  $\mathcal{R}[g]$  over the right interval  $c_{-1}/c_0 < x \leq 1$ , it is actually a composition of the left half  $g_l = g|_{[0, c_0]}$  of the map with the right half  $g_r = g|_{(c_0, 1]}$  of the map, i.e.,

$$\frac{1}{c_0} g \circ g(c_0 x) = \frac{1}{c_0} g_r \circ g_l(c_0 x), \quad \text{for } \frac{c_{-1}}{c_0} \leq x \leq 1.$$

Describing it in words, one iterates  $g$  twice over the interval  $(c_{-1}, c_0)$  and scale the iterated graph over  $(c_{-1}, c_0)$  and  $[0, c_{-1})$  to the unit interval  $[0, 1]$  by the factor  $1/c_0$ . Fig. 3 gives an illustration of the renormalization operation. In terms of the Poincaré map  $f_\mu$  defined from Fig. 1(b), the renormalized element  $\mathcal{R}[f_\mu]$  is the same as the flow induced Poincaré return map on the shorter interval  $[0, c]$ , modulo a rescaling constant. This means regardless the size of the domain of definition one chooses to define ones Poincaré return map, sooner or later a renormalized iterate  $\mathcal{R}^n[f_\mu]$  for some  $n$  will capture it. Two immediate properties are collected by two propositions below with the first characterizing the range and the second the iterates of  $\mathcal{R}$ .

**Proposition 2.** Let  $R = \{g \in Y : g(c_0) = 1\}$ . Then,  $\mathcal{R}[D] = R$ .

**Proof.** For any  $g \in R$ , we need to construct an  $h \in D$  such that  $g = \mathcal{R}[h]$ . To this end, we need to define a scale down operation which is an inverse operation to  $\mathcal{R}$  over a sub-interval immediately left to the point of discontinuity. More specifically, for any  $0 < d < 1$  and every  $g \in R$ , denote

$$S_d[g](x) = dg\left(\frac{1}{d}x\right), \quad 0 \leq x \leq dc_0.$$

Now let

$$c_0^h := \frac{1}{2 - c_0}$$



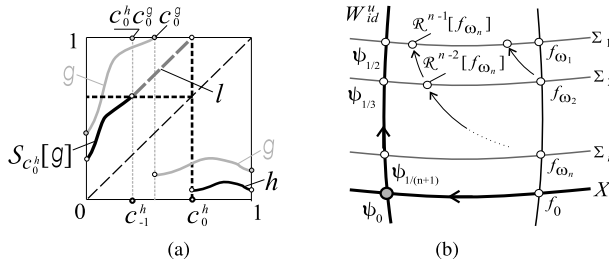


**Fig. 4.** (a) The preimage  $h$  of  $g$  is constructed by scaling  $g$  down ( $S_{c_0^h}[g]$ ), attaching a line segment  $l$  of slope 1, and scaling the right half of  $g$  accordingly over the right interval of  $h$ . (b) A geometric view of the dynamics near the fixed point  $\psi_0$ . Notice that the closer  $f_{\omega_n}$  is to  $X$ , the closer  $\mathcal{R}^{n-1}[f_{\omega_n}]$  is to the point  $\psi_{1/2}$  on  $U = W_{id}^u$ . See also Fig. 5.

and define

$$h(x) := \begin{cases} S_{c_0^h}[g](x) = c_0^h g(\frac{1}{c_0^h}x), & 0 \leq x < c_0^h, \\ l(x) = (x - c_0^h) + c_0^h, & c_0^h \leq x < c_1^h, \\ c_0^h g(\frac{1-c_0}{1-c_0^h}(x - c_0^h) + c_0), & c_0^h \leq x \leq 1. \end{cases} \quad (6)$$

Fig. 4(a) illustrates the construction of  $h$ . It is straightforward to verify that  $c_{-1}^h = c_0 c_0^h$  since  $h(c_{-1}^h) = l(c_{-1}^h) = c_0^h$ ;  $S_{c_0^h}[g](c_{-1}^h) = c_0^h g(c_0) = c_0^h = l(c_{-1}^h)$ ;  $\frac{1}{c_0^h} h(c_0^h x) = g(x)$  for  $x \in [0, c_0]$ ;  $\frac{1}{c_0^h} h \circ h(c_0^h x) = g(x)$  for  $x \in [c_0, 1]$ , and  $h(c_0^h) = 1$ , both using that  $c_0^h = 1/(2 - c_0)$ . Hence  $\mathcal{R}[h] = g$ .  $\square$

**Proposition 3.** For integer  $k \geq 0$  if  $\mathcal{R}^{k-1}[g] \in D$  is renormalizable, then

$$\mathcal{R}^k[g](x) = \begin{cases} \frac{1}{c_{-k+1}} g(c_{-k+1}x), & 0 \leq x < \frac{c_{-k}}{c_{-k+1}}, \\ \frac{1}{c_{-k+1}} g^{k+1}(c_{-k+1}x), & \frac{c_{-k}}{c_{-k+1}} \leq x \leq 1, \end{cases}$$

where  $c_{-i} = g^{-i}(c_0) \in [0, c_0]$  for all  $i = 0, 1, \dots, k$ . More specifically, if  $c_0$  has  $n$  backward iterates  $c_{-i} = g^{-i} \in [0, c_0]$  for  $i = 1, \dots, n$ , then the new point  $c_{-1}/c_0$  which partitions the graph of  $\mathcal{R}[g]$  into parts above the diagonal and below the point  $c_{-1}/c_0$  has  $n - 1$  backward iterates  $c_{-j-1}/c_0 = \mathcal{R}[g]^{-j}(c_{-1}/c_0)$  in  $[0, c_{-1}/c_0]$  for  $j = 1, \dots, n - 1$ .

**Proof.** It follows by induction.  $\square$

A subset  $U \subset D$  is forward invariant if  $\mathcal{R}[U] \subset U$ . It is backward invariant if there is a subset  $V \subset U$  such that  $\mathcal{R}[V] = U$ . It is invariant if it is both forward and backward invariant, i.e.,  $\mathcal{R}[U] = U$ .

**Proposition 4.** Let

$$X = \{g \in Y : \exists x_* \in [0, c_0] \text{ such that } g(x_*^-) = x_*\},$$

$$\Sigma_n = \{g \in R \subset Y : g^{-k}(c_0) = c_{-k} \in [0, c_0] \text{ for } 1 \leq k \leq n \text{ such that } 0 = c_{-n} < c_{-n+1} < \dots < c_0\},$$

where  $g(x_*^-) = \lim_{x \rightarrow x_*^-} g(x)$ . Then

(a)  $X \subset D$  is forward invariant and  $\mathcal{R}[X]$  is invariant, i.e.,  $\mathcal{R}^2[X] = \mathcal{R}[X]$ .

- (b)  $X$  contains all forward invariant subsets of  $Y$  under  $\mathcal{R}$ .
- (c)  $\Sigma_{n+1} = \mathcal{R}^{-n}[\Sigma_1]$  and more generally,  $\mathcal{R}^k[\Sigma_{n+k}] = \Sigma_n$ .

**Proof.** For  $g \in X$ , let  $x_g = \sup\{x_* \in [0, c_0] : x_* = g(x_*^-)\}$ . Then we also have  $x_g = g(x_g^-)$ . So without loss of generality, assume  $x_* = x_g$  is the largest fixed point of  $g$  in  $[0, c_0]$  for statement (a). If  $x_* < c_0$ , then  $g(x) > x$  for  $x_* < x \leq c_0$ . So  $c_k = g^{-k}(c_0)$  exist for all  $k \geq 1$  and  $c_0 > c_{-1} > \dots \rightarrow x_*$ . Thus  $g \in D$  and  $\mathcal{R}[g] \in X$  with the scaled fixed point  $x_*/c_0$ . If  $x_* = c_0$ , then  $\mathcal{R}[g]$  has 1 as its fixed point. In either cases we have  $\mathcal{R}[g] \in X$  and  $X$  is forward invariant. Hence,  $\mathcal{R}^2[X] \subset \mathcal{R}[X] \subset X$ . To show  $\mathcal{R}[X]$  is backward invariant, take any  $g \in \mathcal{R}[X] \subset R = \mathcal{R}[D]$ . By Proposition 2 there is an  $h \in D$  such that  $\mathcal{R}[h] = g$ . By the construction of  $h$  from (6), we see that  $h$  has a scaled-down fixed point  $x_*c_0^h$ . Thus,  $h \in X$ . Since  $h(c_0^h) = 1$  from the construction in Proposition 2, we have  $h \in R$  and  $h \in \mathcal{R}[X]$ . Hence, (a) holds.

If  $g \in U$  and  $U$  is forward invariant, then  $\mathcal{R}^k[g]$  exists for all  $k \geq 0$ . That is,  $g^{-k}(c_0) = c_{-k}$  exist for all  $k \geq 1$  with  $0 \leq \dots < c_{-k} \leq c_{-k+1} \leq \dots \leq c_0$ . Thus  $\lim_{k \rightarrow \infty} c_k = x_* \in [0, c_0]$  exists and  $g(x_*) = x_*$ . So  $g \in X$  and  $U \subset X$  holds. This shows (b).

If  $g \in \Sigma_{n+1}$ , then  $0 = c_{-n-1} \leq c_{-n} \leq \dots \leq c_{-1} \leq c_0$ . By Proposition 3,  $\mathcal{R}^n[g]$  exists with the discontinuity at  $c_{-n}/c_{-n+1}$  and the discontinuity's preimage at  $c_{-n-1}/c_{-n+1} = 0$ . This shows  $\mathcal{R}^n[g] \in \Sigma_1$  by definition. Thus,  $\Sigma_{n+1} \subset \mathcal{R}^{-n}[\Sigma_1]$ . To show  $\Sigma_{n+1} \supset \mathcal{R}^{-n}[\Sigma_1]$ , we need to show that for any  $g \in \Sigma_1$ , there is an  $\tilde{h} \in \Sigma_{n+1}$  such that  $\mathcal{R}^n[\tilde{h}] = g$ . Since  $g \in \Sigma_1 \subset R$ , we can construct an  $h$  by (6) of Proposition 2 for which  $\mathcal{R}[h] = g$ . From the construction of  $h$  we can conclude that  $c_0^h = 1/(2 - c_0^g)$ ,  $c_{-1}^h = c_0^g c_0^h$ , and  $c_{-2}^h = c_{-1}^g c_0^h = 0$  since  $g \in \Sigma_1$ . Also,  $h(c_0^h) = 1$ . So  $h \in \Sigma_2$ . Applying the same inverse procedure to  $h$  recursively we can find  $\tilde{h} \in \Sigma_{n+1}$  such that  $\mathcal{R}^n[\tilde{h}] = g$ . So  $\Sigma_{n+1} \supset \mathcal{R}^{-n}[\Sigma_1]$ . The general identity of (c) can be verified similarly. This completes (c).  $\square$

The following result simply says that  $\{\Sigma_n\}$  converges to  $X$  point-wise uniformly over  $[0, 1]$ .

**Proposition 5.** For each  $g \in X$ , there is a sequence  $g_n \in \Sigma_n$  such that  $g_n \rightarrow g$  uniformly in  $[0, 1]$ .

**Proof.** Let  $g \in X$ . Define

$$g_\mu(x) := \begin{cases} g(x), & \text{when } g(x) \geq x + \mu \text{ and } x \in [0, c_0], \\ x + \mu, & \text{when } g(x) \leq x + \mu \text{ and } x \in [0, c_0], \\ g(x), & x \in (c_0, 1]. \end{cases}$$

It is straightforward to verify that  $g_\mu(x) > x$  for small  $\mu > 0$  for  $x \in [0, c_0]$ . By intermediate value theorem there exists a decreasing sequence  $\{\mu_n\}$  for sufficiently large  $n$  such that  $\mu_n \rightarrow 0$  and  $g_{\mu_n}^n(0) = c_0$ , i.e.,  $g_{\mu_n} \in \Sigma_n$ . The convergence that  $g_{\mu_n} \rightarrow g$  is obviously uniformly over the interval  $[0, 1]$ .  $\square$

**Proposition 6.** Let

$$W_{id}^u := \{\psi_\mu : 0 \leq \mu \leq 1/2\} \quad \text{with } \psi_\mu(x) = \begin{cases} \mu + x, & 0 \leq x < 1 - \mu, \\ 0, & 1 - \mu \leq x \leq 1. \end{cases}$$

Then

- (a)  $id = \psi_0$  is a fixed point of  $\mathcal{R}$ .
- (b)  $W_{id}^u$  is backward invariant with  $\mathcal{R}[\psi_\mu] = \psi_{\mu/(1-\mu)}$ .
- (c)  $\mathcal{R}$  is weakly expanding along  $W_{id}^u$  in the sense that

$$\|\mathcal{R}[\psi_\mu] - \psi_0\| > \|\psi_\mu - \psi_0\|.$$

(d) 1 is an eigenvalue of  $\mathcal{R}$ 's linearization at  $\psi_0$  and the unit eigenvector is given as

$$u_0(x) := \frac{1}{2}s_1(x) - \frac{1}{2}\delta_1(x),$$

where  $s_1(x) = 1, 0 \leq x < 1$ , and  $s_1(1) = 0$ , i.e.  $s_1 \equiv 1$  in  $L^1$ , and  $\delta_1$  is the delta distribution function, i.e.,  $\delta_1(x) = 0, x \neq 1, \delta_1(1) = \infty$ , and  $\int_{1-a}^{1+a} \phi(x)\delta_1(x) dx = \phi(1)$  for any  $C^0$  test function  $\phi$ , and any  $0 < a \leq \infty$ .

**Proof.** It is straightforward to verify (a) as well as (b):

$$\mathcal{R}[\psi_\mu] = \psi_{\mu/(1-\mu)}, \quad \text{and equivalently, } \mathcal{R}^{-1}[\psi_\mu] = \psi_{\mu/(1+\mu)}.$$

It is not forward invariant because it requires  $\mu/(1-\mu) < 1/2$ , or  $\mu < 1/3$ . That is, with  $V = \{\psi_\mu: 0 \leq \mu < 1/3\} \subset W_{id}^u$  we have  $\mathcal{R}[V] = W_{id}^u$ .

To show (c), a more general relation holds as follows

$$\|\psi_\mu - \psi_0\| > \|\psi_\zeta - \psi_0\| \quad \text{if } \mu > \zeta \geq 0.$$

In fact, since in general  $\|\psi_\mu - \psi_\lambda\|$  is the area between the two curves that consists of the area of a parallelogram and the area of a trapezoid, we have thus by elementary calculations

$$\|\psi_\mu - \psi_\lambda\| = (\mu - \lambda) \left( \frac{4 + \lambda - 3\mu}{2} \right) \sim (\mu - \lambda), \quad \text{assuming } \mu > \lambda \geq 0. \tag{7}$$

In particular, with  $\lambda = 0$ , we have

$$\|\psi_\mu - \psi_0\| = \mu \frac{4 - 3\mu}{2},$$

which is increasing in  $\mu \in [0, 2/3] \supset [0, 1/2]$ . Since  $\mathcal{R}[\psi_\mu] = \psi_{\mu/(1-\mu)}$  by (b), (c) is verified.

Again by (b) and expression (7), we have

$$\begin{aligned} \|\mathcal{R}[\psi_\mu] - \mathcal{R}[\psi_0] - 1 \cdot (\psi_\mu - \psi_0)\| &= \|\psi_{\mu/(1-\mu)} - \psi_\mu\| \\ &= \left( \frac{\mu}{1-\mu} - \mu \right) \frac{4 - 3\mu}{2} \sim \mu^2 \sim \|\psi_\mu - \psi_0\|^2, \end{aligned}$$

showing the derivative of  $\mathcal{R}$  at  $\psi_0$  in the direction of  $W_{id}^u$  is the unitary operator in  $L^1$ , and 1 is the eigenvalue. As for the unit eigenvector  $u_0$  we have

$$\begin{aligned} u_\mu &:= \frac{\psi_\mu - \psi_0}{\|\psi_\mu - \psi_0\|} = \begin{cases} \frac{2}{4-3\mu}, & 0 \leq x < 1 - \mu, \\ \frac{-2x}{\mu(4-3\mu)}, & 1 - \mu < x \leq 1, \end{cases} \\ &= \begin{cases} \frac{2}{4-3\mu}, & 0 \leq x < 1 - \mu, \\ 0, & 1 - \mu < x \leq 1, \end{cases} + \begin{cases} 0, & 0 \leq x < 1 - \mu, \\ \frac{-2x}{\mu(4-3\mu)}, & 1 - \mu < x \leq 1, \end{cases} \\ &\rightarrow \frac{1}{2}s_1(x) - \frac{1}{2}\delta_1(x) = u_0(x), \quad \text{as } \mu \rightarrow 0. \end{aligned}$$

This proves (d).  $\square$

**Proposition 7.**

- (a)  $\gamma = \{\psi_{1/n}\}$ ,  $n \geq 2$ , is a backward orbit of  $\mathcal{R}$  starting at  $\psi_{1/2}$ .
- (b)  $\psi_\mu^n(0) = c_0 = 1 - \mu$  if and only if  $\mu = 1/(n + 1)$ , i.e.,  $\psi_{1/(n+1)} \in \Sigma_n$ .
- (c)  $\omega_n = \alpha_{n+1} = 1/(n + 1)$ , that is,  $\psi_\mu$  is isospiking of length  $n$  if and only if  $1/(n + 1) \leq \mu < 1/n$ .

(d) 
$$\frac{\omega_{n+1} - \omega_{n+2}}{\omega_n - \omega_{n+1}} = 1 - \frac{2}{n} + h.o.t. \rightarrow 1 \quad \text{as } n \rightarrow \infty.$$

(e) 
$$\|\psi_{1/n} - \psi_0\| = \frac{1}{n} \left( 2 - \frac{3}{2n} \right), \quad \text{and}$$

$$\begin{aligned} \frac{\|\psi_{1/(n+2)} - \psi_{1/(n+1)}\|}{\|\psi_{1/(n+1)} - \psi_{1/n}\|} &= 1 - \frac{2}{n+2} + h.o.t. \\ &= 1 - \frac{2}{n} + h.o.t. \rightarrow 1 \quad \text{as } n \rightarrow \infty. \end{aligned}$$

**Proof.** Statement (a) holds because by the proof of Proposition 6 we have  $\mathcal{R}[\psi_\mu] = \psi_{\mu/(1-\mu)}$  and the identity

$$\frac{\frac{1}{n}}{1 + \frac{1}{n}} = \frac{1}{n + 1}.$$

Statement (b) holds because  $\psi_\mu^n(0) = n\mu = c_0 = 1 - \mu$  iff  $\mu = 1/(n + 1)$ . Statement (c) follows from the isospiking criterion of Section 3. Statement (d) is straightforward. Finally, (e) follows from the expression (7).  $\square$

Notice that by the expression (7),  $\|\psi_{1/(n+1)} - \psi_{1/n}\| \sim (1/n - 1/(n + 1)) = \omega_{n-1} - \omega_n$ . Thus (d) and (e) are essentially the same. Also statement (e) reconfirms the fact that 1 is the eigenvalue along the direction  $W_{id}^\mu$  and taking the limit of the quotient difference

$$\frac{\omega_{n+1} - \omega_{n+2}}{\omega_n - \omega_{n+1}} \rightarrow 1$$

is an approximation scheme for the eigenvalue.

**Theorem of Universal Number 1.** Let  $\{f_\mu\}$  with  $0 \leq \mu \leq m_0 \ll 1$  be a one-parameter family in  $Y$ , where  $m_0$  is a sufficiently small constant and  $f_\mu \in Y$  for all  $\mu \in [0, m_0]$ . Let  $c_0^\mu = c_0^{f_\mu} \in (0, 1]$  with  $\mu \in [0, m_0]$  denote the discontinuity of  $f_\mu$  and  $c_{-k}^\mu = f_\mu^{-k}(c_0^\mu)$  be the  $k$ th back iterate of  $c_0^\mu$ . Assume the following conditions are satisfied:

- (a) There exist an integer  $k_0 \geq 1$  and a constant  $c_1$  such that

$$c_{-k_0+1}^\mu = c_0^0 + c_1\mu + o(\mu)$$

for  $\mu \in [0, m_0]$ .

- (b) There exist some constants  $a_1 > 0, a_2$  such that

$$f_\mu(x) = x + a_1\mu + a_2\mu^2 + o(\mu^2) \quad \text{for } x \in [0, c_{-k_0}^\mu] \text{ and } \mu \in [0, m_0].$$

Then there exists a unique monotone decreasing sequence  $\{\omega_n\}$  with  $\omega_n \rightarrow 0$  such that

$$f_{\omega_n} \in \Sigma_n \quad \text{and} \quad \frac{\omega_{n+1} - \omega_{n+2}}{\omega_n - \omega_{n+1}} \rightarrow 1 \quad \text{as } n \rightarrow \infty. \tag{8}$$

More generally, for any pair of integers  $p \geq 0$  and  $q > 0$  we have

$$\frac{\omega_{n+q} - \omega_{n+q+p}}{\omega_n - \omega_{n+q}} \rightarrow \frac{p}{q} \quad \text{as } n \rightarrow \infty. \tag{9}$$

**Remark.** By the assumptions (a), (b) above, neural families are distinguished by the parameters  $c_0^\mu$ ,  $c_1$ ,  $a_1$ ,  $a_2$ , and the higher order terms in their expansion at  $\mu = 0$ . They all share the same property that  $f_\mu(x) \rightarrow x$  as  $\mu \rightarrow 0$ , which is the main cause for the stated universality.

**Proof.** The proof will be done by mainly considering the  $k_0$ th renormalized family  $g_\mu = \mathcal{R}^{k_0}[f_\mu]$ . Consider  $g_\mu(x)$  in the left half interval  $x \in [0, \bar{c}_0^\mu]$  only, we have by Proposition 3 and both hypotheses (a), (b),

$$g_\mu(x) = x + \frac{1}{c_{-k_0+1}^\mu} (a_1\mu + a_2\mu^2 + o(\mu^2)) = x + \bar{a}_1\mu + \bar{a}_2\mu^2 + o(\mu^2)$$

where  $\bar{a}_1 = a_1/c_0^0 > 0$  and  $\bar{a}_2$  is a constant depending on  $a_1$ ,  $a_2$ ,  $c_0^0$ ,  $c_1$ , obtained by collecting the coefficients of  $\mu$ -term and  $\mu^2$ -term respectively in  $g_\mu$ . Denote the discontinuity of  $g_\mu$  by

$$\bar{c}_0^\mu = \frac{c_{-k_0}^\mu}{c_{-k_0+1}^\mu}.$$

Then from the expression of  $g_\mu$  and the equation  $g_\mu(\bar{c}_0^\mu) = 1$  we obtain

$$\bar{c}_0^\mu = 1 - (\bar{a}_1\mu + \bar{a}_2\mu^2 + o(\mu^2)) := 1 + b_1\mu + o(\mu),$$

where  $b_1 = -\bar{a}_1$ .

By definition,  $g_\mu \in \Sigma_n$  if and only if  $g_\mu^n(0) = \bar{c}_0^\mu = 1 + b_1\mu + o(\mu)$ . It is by induction to get

$$g_\mu^n(0) = n(\bar{a}_1\mu + \bar{a}_2\mu^2 + o(\mu^2)).$$

Thus solving  $g_\mu^n(0) = \bar{c}_0^\mu$  is equivalent to solving

$$\theta(\mu) := g_\mu^n(0) - \bar{c}_0^\mu = n(\bar{a}_1\mu + \bar{a}_2\mu^2 + o(\mu^2)) - (1 + b_1\mu + o(\mu)) = 0.$$

This is done by showing that for each sufficiently large  $n$ ,  $\theta$  is increasing in  $\mu$  with the property that  $\theta(0) = -1 < 0$  and  $\theta(m_0) > 0$ . Therefore there is a unique solution denoted by

$$\mu = \bar{\omega}_n.$$

To approximate  $\bar{\omega}_n$ , we assume it takes the following form

$$\bar{\omega}_n = \frac{r_1}{n} + \frac{r_2}{n^2} + o\left(\frac{1}{n^2}\right).$$

Substituting this form into the equation  $g_\mu^n(0) = \tilde{c}_0^\mu$ , approximating the equation to order  $o(\frac{1}{n})$  by equating the constant and  $1/n$  terms on both sides, we find

$$r_1 = \frac{1}{\bar{a}_1} \quad \text{and} \quad r_2 = \frac{b_1 r_1 - \bar{a}_2 r_1^2}{\bar{a}_1}.$$

Now for any integer pair  $p \geq 0$  and  $q > 0$  we have by elementary simplification

$$\begin{aligned} \frac{\bar{\omega}_{n+q} - \bar{\omega}_{n+q+p}}{\bar{\omega}_n - \bar{\omega}_{n+q}} &= \frac{\frac{r_1}{n+q} + \frac{r_2}{(n+q)^2} + o(\frac{1}{n^2}) - (\frac{r_1}{n+q+p} + \frac{r_2}{(n+q+p)^2} + o(\frac{1}{n^2}))}{\frac{r_1}{n} + \frac{r_2}{n^2} + o(\frac{1}{n^2}) - (\frac{r_1}{n+q} + \frac{r_2}{(n+q)^2} + o(\frac{1}{n^2}))} \\ &= \frac{n(n+q)}{(n+q)(n+q+p)} \frac{pr_1 + r_2 \frac{p(2n+2q+p)}{(n+q)(n+p+q)} + o(1)}{qr_1 + r_2 \frac{q(2n+q)}{n(n+q)} + o(1)} \\ &\rightarrow \frac{p}{q} \quad \text{as } n \rightarrow \infty. \end{aligned}$$

Finally, we notice that due to renormalization,  $g_\mu = \mathcal{R}^{k_0}[f_\mu] \in \Sigma_n$  if and only if  $f_\mu \in \Sigma_{n+k_0}$  by Proposition 4. Therefore we can conclude that  $\omega_{n+k_0} = \bar{\omega}_n$  and the limit

$$\frac{\omega_{n+q} - \omega_{n+q+p}}{\omega_n - \omega_{n+q}} \rightarrow \frac{p}{q} \quad \text{as } n \rightarrow \infty$$

holds as desired. This proves the theorem.  $\square$

**Proposition 8.** *The universality (8) implies the universality (9).*

**Proof.** In fact, the limit (8) implies the following two limits: For any fixed integers  $m \geq 0, k > 0$ , we have

$$\frac{\omega_{n+m} - \omega_{n+m+1}}{\omega_n - \omega_{n+1}} = \prod_{i=1}^m \frac{\omega_{n+i} - \omega_{n+i+1}}{\omega_n + (i-1) - \omega_{n+i}} \rightarrow \prod_{i=1}^m 1 \quad \text{as } n \rightarrow \infty,$$

and

$$\frac{\omega_{n+m} - \omega_{n+m+k}}{\omega_n - \omega_{n+1}} = \sum_{j=0}^{k-1} \frac{\omega_{n+m+j} - \omega_{n+m+j+1}}{\omega_n - \omega_{n+1}} \rightarrow \sum_{j=0}^{k-1} 1 = k \quad \text{as } n \rightarrow \infty.$$

Hence, we have the universality limit (9):

$$\frac{\omega_{n+q} - \omega_{n+q+p}}{\omega_n - \omega_{n+q}} = \frac{(\omega_{n+q} - \omega_{n+q+p})/(\omega_n - \omega_{n+1})}{(\omega_n - \omega_{n+q})/(\omega_n - \omega_{n+1})} \rightarrow \frac{p}{q} \quad \text{as } n \rightarrow \infty. \quad \square$$

We note that  $X$  contains  $id = \psi_0$  and is forward invariant. It is large enough to contain infinitely many co-dimension-one subspaces of  $Y$ . For example, let  $E_{x_0} : Y \rightarrow \mathbb{R}$  be the functional such that  $E_{x_0}(g) = g(x_0) - x_0$ . Then the subspace  $\{g \in Y : E_{x_0}(g) = 0\}$  is at least of co-dimension-one in  $X$ . On the other hand,  $W_{id}^u$  is a 1-dimensional manifold that is not in  $X$ . So  $X$  is a subset of  $Y$  that is not smaller than co-dimension-one space but smaller than the full space. In any case,  $X$  is the center-stable set and  $W_{id}^u$  is the (weak) unstable manifold of the non-hyperbolic fixed point  $id = \psi_0$ . Thus,

similar to  $\lambda$ -lemmas of non-hyperbolic fixed points from [5], we should expect the following: For any continuous one-parameter family  $\{f_\mu\} \subset Y$  of mappings that intersects the stable set  $X$  transversely at  $f_0$ , if  $\mathcal{R}^n[f_0] \rightarrow id = \psi_0$ , then  $\mathcal{R}^n[\{f_\mu\}]$  must converge to the unstable manifold  $W_{id}^u$  as  $n \rightarrow \infty$ . The following result is a weaker form of such  $\lambda$ -lemmas.

**Inclination lemma.** Let  $\{f_\mu\}$  with  $0 \leq \mu \leq m_0 \ll 1$  be a one-parameter family in  $Y$ , where  $m_0$  is a sufficiently small constant and  $f_\mu \in Y$  for all  $\mu \in [0, m_0]$ . Let  $c_0^\mu = c_0^{f_\mu} \in (0, 1]$  with  $\mu \in [0, m_0]$  denote the discontinuity of  $f_\mu$  and  $c_{-k}^\mu = f_\mu^{-k}(c_0^\mu)$  be the  $k$ th back iterate of  $c_0^\mu$ . Assume the following conditions are satisfied:

(a) There exist an integer  $k_0 \geq 1$  and a constant  $c_1$  such that

$$c_{-k_0+1}^\mu = c_0^\mu + c_1\mu + o(\mu)$$

for  $\mu \in [0, m_0]$ .

(b) There exists a constant  $a_1 > 0$  such that

$$f_\mu(x) = x + a_1\mu + o(\mu) \quad \text{for } x \in [0, c_{-k_0}^\mu] \text{ and } \mu \in [0, m_0].$$

(c)  $f_\mu(x) = O(\mu)$  for  $x \in (c_0^\mu, 1]$  and  $\mu \in [0, m_0]$ .

Then for any  $\mu_0$ , and any  $\epsilon > 0$ , there is an integer  $N_0$  such that for any iterate  $n > N_0$ , there is a  $\mu \in (0, m_0]$  sufficiently small satisfying the following

$$\|\mathcal{R}^n[f_\mu] - \psi_{\mu_0}\| < \epsilon,$$

where  $\psi_\mu$  defines the backward invariant, expanding family through  $id$  constructed in Proposition 6.

**Proof.** Fig. 4(b) gives an illustration for the lemma. Similar to the proof of the Theorem of Universal Number 1, the proof is carried out by considering the  $k_0$ th renormalized family  $g_\mu = \mathcal{R}^{k_0}[f_\mu]$ . Denote the discontinuity of  $g_\mu$  by  $\bar{c}_0^\mu$ . By Proposition 3 and hypotheses (a), (c), we have

$$g_\mu(x) = O(\mu) \quad \text{for } x \in (\bar{c}_0^\mu, 1] \text{ and } \mu \in [0, m_0],$$

because the outer most composition in  $f_\mu^{k_0+1}(c_{-k_0+1}^\mu)/c_{-k_0+1}^\mu$  is of order  $O(\mu)$  and  $c_{-k_0+1}^\mu = O(1)$ . Consider  $g_\mu(x)$  in the left half interval  $x \in [0, \bar{c}_0^\mu]$  next, we have by Proposition 3 and both hypotheses (a), (b),

$$g_\mu(x) = x + \frac{1}{c_{-k_0+1}^\mu} (a_1\mu + o(\mu)) = x + \bar{a}_1\mu + o(\mu)$$

where  $\bar{a}_1 = a_1/c_0^0 > 0$  is a constant similar to the proof of the preceding theorem. Denote

$$\bar{c}_{-k}^\mu = g_\mu^{-k}(\bar{c}_0^\mu),$$

whenever defined. For simpler notation we denote

$$c_{-k} = \bar{c}_{-k}^\mu \quad \text{for } k = 0, 1, 2, \dots, \quad \text{and} \quad a = \bar{a}_1.$$

Since  $g_\mu \in \mathcal{R}[D] = R$ ,  $g_\mu(c_0) = 1$  (using the simplified notation  $c_0 = \bar{c}_0^\mu$ ), and thus

$$g_\mu^{k+1}(c_{-k}) = c_{-k} + (k + 1)(a\mu + o(\mu)) = 1.$$

Thus

$$c_{-k} = 1 - (k + 1)(a\mu + o(\mu)) \quad \text{and} \quad c_0 = 1 - (a\mu + o(\mu)).$$

By Proposition 3,

$$\mathcal{R}^k[g_\mu](x) = x + \frac{a\mu + o(\mu)}{c_{-k+1}} \quad \text{for } 0 \leq x \leq \frac{c_{-k}}{c_{-k+1}}.$$

The rest of the proof is to show that a  $\mu$  satisfying the following equation

$$\frac{a\mu}{c_{-k+1}} = \mu_0 \tag{10}$$

is what we look for. By using the expression for  $c_{-k}$ , the equation above is solved to give

$$\mu = \frac{\mu_0}{a + k\mu_0(a + o(1))} = O\left(\frac{1}{k}\right) \rightarrow 0 \quad \text{as } k \rightarrow \infty.$$

We are now ready to estimate  $\|\mathcal{R}^k[g] - \psi_{\mu_0}\|$ . The difference is the area between the two curves  $h = \mathcal{R}^k[g_\mu]$  and  $\psi_{\mu_0}$  which can be divided into three regions for consideration: (i) The parallelogram between  $h = \mathcal{R}^k[g_\mu]$  and  $\psi_{\mu_0}$  over the interval  $[0, \min\{c_0^h, 1 - \mu_0\}]$ ; (ii) the trapezoid-like region between the two curves over the interval  $[\min\{c_0^h, 1 - \mu_0\}, \max\{c_0^h, 1 - \mu_0\}]$ ; (iii) the region between  $h$  and the  $x$ -axis over the interval  $[\max\{c_0^h, 1 - \mu_0\}, 1]$  for which the height of the curve  $h$  is of order  $O(\mu)$ . Our task is to show that each of the three areas is of order  $o(1)$  as  $\mu = O(1/k) \rightarrow 0$ . First there is no additional argument needed for the region (iii) because  $h = O(\mu)$  over the corresponding sub-interval of  $[0, 1]$ . For region (i), because of the choice of  $\mu$  from the equation  $a\mu/c_{-k+1} = \mu_0$ , we have that the difference between the two curves  $h$  and  $\psi_{\mu_0}$  over that interval is

$$\begin{aligned} |h(x) - \psi_{\mu_0}| &= \left| \frac{a\mu + o(\mu)}{c_{-k+1}} - \mu_0 \right| = \frac{o(\mu)}{c_{-k+1}} \\ &= \frac{a\mu}{c_{-k+1}} \frac{o(\mu)}{a\mu} = \mu_0 o(1) \quad \left( \text{because } \frac{a\mu}{c_{-k+1}} = \mu_0 \text{ by Eq. (10)} \right) \\ &= o(1) \quad \text{as } \mu \rightarrow 0. \end{aligned}$$

For region (ii), the function difference between  $h$  and  $\psi_{\mu_0}$  is of order  $O(1)$ . However, the length of the interval  $[\min\{c_0^h, 1 - \mu_0\}, \max\{c_0^h, 1 - \mu_0\}]$  is small. In fact, the length of the interval is

$$\begin{aligned} |c_0^h - 1 + \mu_0| &= \left| \frac{c_{-k}}{c_{-k+1}} - 1 + \mu_0 \right| = \left| \frac{c_{-k} - c_{-k+1} + \mu_0 c_{-k+1}}{c_{-k+1}} \right| \\ &= \left| \frac{c_{-k} - c_{-k+1} + a\mu}{c_{-k+1}} \right| \quad \left( \text{because } \mu_0 c_{-k+1} = a\mu \text{ by Eq. (10)} \right) \\ &= \left| \frac{-a\mu - o(\mu) - a\mu}{c_{-k+1}} \right| \quad \left( \text{because } c_{-k+1} = g_\mu(c_{-k}) = c_{-k} + a\mu + o(\mu) \right) \\ &= \left| \frac{o(\mu)}{c_{-k+1}} \right| = o(1), \end{aligned}$$



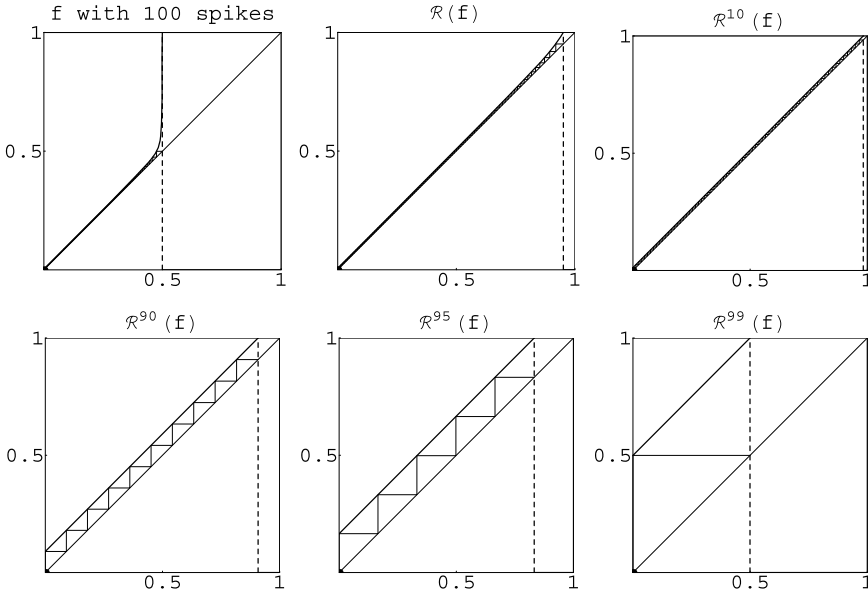


**Fig. 5.** A spike map  $f$  which initially can generate 100 spikes is far away from the fixed point  $\psi_0$  at the start of the renormalization. Then  $\mathcal{R}(f)$  moves closer to  $\psi_0$ , but  $\mathcal{R}^{10}(f)$  closer still before the last three iterates move farther from the fixed element  $\psi_0$ .

where the last estimate follows from the same argument as above for region (i). Combining the three estimates together, we can conclude that

$$\|\mathcal{R}^k[g_\mu] - \psi_{\mu_0}\| = o(1) \quad \text{as } \mu = O\left(\frac{1}{k}\right) \rightarrow 0.$$

Hence, there exists a sufficiently large  $K_0$  so that for  $k > K_0$  we have

$$\|\mathcal{R}^k[g_\mu] - \psi_{\mu_0}\| < \epsilon$$

for  $\mu$  defined as in Eq. (10). Since  $\mathcal{R}^k[g_\mu] = \mathcal{R}^{k+k_0}[f_\mu]$ , the lemma is proved by choosing  $N_0 = K_0 + k_0$ .  $\square$

The dynamical structure of  $\mathcal{R}$  near  $\psi_0 = id$  can be seen by a simulation by the iterates of  $\mathcal{R}$  on a spike map  $f$  shown in Fig. 5. The weakly saddle structure near the fixed point  $id$  is clearly evident when the iterates are shown in their graphs as functions of the unit interval.

We end this section with some other backward invariant weakly-expanding families through the fixed point  $id = \psi_0$ . They are similar to  $\psi_\mu$  except for the non-vanishing part of the refractory interval. More specifically, consider families of the following form

$$g_{\mu,q}(x) = \begin{cases} x + \mu, & 0 \leq x < 1 - \mu, \\ q_\mu(x), & 1 - \mu \leq x \leq 1, \end{cases}$$

where  $q_\mu(x) \geq 0$  and  $\max_{[1-\mu,1]} q_\mu \leq \mu$ . It is straightforward to verify that the set  $W_{id,q}^u := \{g_{\mu,q} : 0 \leq \mu < 1/2\}$  is backward invariant if and only if

$$q_{\frac{\mu}{1-\mu}}(x) = \frac{1}{1-\mu} q_{\mu}((1-\mu)x + \mu), \quad \frac{1-2\mu}{1-\mu} \leq x \leq 1.$$

For example, consider  $q_{\mu}$  to be the logistic family  $q_{\mu} = 4\lambda(x-1+\mu)(x-1)$ . The  $x$ -intercepts are  $x = 1 - \mu = c_0$  and  $x = 1$ . The maximum takes place at  $1 - \mu/2$  with  $\lambda\mu$  the maximum value. Because  $g_{\mu,q}$  is linear on the left half interval  $[0, c_0] = [0, 1 - \mu]$ , the renormalization  $\mathcal{R}[g_{\mu,q}]$  on the right half interval  $[(1-2\mu)/(1-\mu), 1]$  is again a quadratic function which goes through the zero at  $x = (1-2\mu)/(1-\mu) = 1 - \mu/(1-\mu)$  and  $x = 1$  respectively and have the maximum value  $\lambda\mu/(1-\mu)$  at  $x = (1 - \mu/2)/(1 - \mu) = 1 - \mu/[2(1 - \mu)]$ . It is precisely the quadratic function  $q_{\mu/(1-\mu)}$ . Thus,  $W_{id,q}^u$  is backward invariant. One can construct other backward invariant families as well, e.g., replacing the logistic family by the tent map family gives rise to such a family. One can also show by the same argument as for Proposition 6 that such a backward invariant family is also tangent to  $u_0$  at the fixed point  $id = \psi_0$ , i.e.,  $\lim_{\mu \rightarrow 0} \frac{g_{\mu,q} - \psi_0}{\|g_{\mu,q} - \psi_0\|} = u_0$ , where  $u_0$  is the eigenvector of eigenvalue 1 as in Proposition 6. One can also show that if  $\min_{x \in [c_0, 1]} q_{\mu}(x) = 0$ , then the same scaling laws as Proposition 7(c,d,e) hold for  $g_{\mu,q}$  as well by exactly the same argument of that proposition. We note also that whether or not a mapping  $g \in F[0, 1]$  is isospiking in its transient dynamics has little to do with its asymptotic dynamics on the interval  $[0, 1]$ . For example, for the family  $\{g_{\mu,q}\}$  with  $q_{\mu} = 4\lambda(x-1+\mu)(x-1)$ , its dynamics is determined by the logistic map. In fact, for  $g_{\omega_n,q} \in \Sigma_n$ ,  $\mathcal{R}^n[g_{\omega_n,q}](x) = \lambda x(1-x)$  is the logistic map. Also, for any fixed  $\mu$ , the bifurcation diagram for  $\{g_{\mu,q}\}$  with varying  $\lambda \in (0, 1)$  is essentially the diagram for the logistic family. Finally, we point out that for the neuron family  $f_{\mu}$  from Fig. 1(b),  $f_{\mu}|_{[c_0, 1]}$  is of order  $\exp(-1/\mu)$ . Thus, the dynamics of each mapping is very much regular. The  $\exp(-1/\mu)$  order estimate over its right interval results in the  $\exp(-n)$  order estimate for the length of the  $n$ th nonisospiking interval,  $|\omega_n - \alpha_{n+1}| \sim \exp(-n)$ , when  $\mu$  is in the nonisospiking interval with  $\mu$  having the same order as that of  $\alpha_n, \omega_n \sim 1/n$ .

We end the paper by pointing out that not only the isospiking universality applies to the circuit models of neurons from [15] but also applies to food chain models from [13], and to any models which share the same spike generating mechanism.

## References

- [1] P. Collet, J.-P. Eckmann, *Iterated Maps of Interval as Dynamical Systems*, Birkhäuser, 1980.
- [2] E. de Faria, W. de Melo, A. Pinto, Global hyperbolicity of renormalization for  $C^r$  unimodal mappings, *Ann. of Math.* 164 (2006) 731–824.
- [3] W. de Melo, S. van Strien, *One-Dimensional Dynamics*, Springer-Verlag, Berlin, 1993.
- [4] B. Deng, The Šil'nikov problem, exponential expansion, strong  $\lambda$ -lemma,  $C^1$ -linearization, and homoclinic bifurcations, *J. Differential Equations* 79 (1989) 189–231.
- [5] B. Deng, Homoclinic bifurcations with nonhyperbolic equilibria, *SIAM J. Math. Anal.* 21 (1990) 693–719.
- [6] B. Deng, A mathematical model that mimics the bursting oscillations in pancreatic  $\beta$ -cells, *Math. Biosci.* 119 (1993) 241–250.
- [7] B. Deng, Constructing homoclinic orbits and chaotic attractors, *Internat. J. Bifur. Chaos Appl. Sci. Engrg.* 4 (1994) 823–841.
- [8] B. Deng, Glucose-induced period-doubling cascade in the electrical activity of pancreatic  $\beta$ -cells, *J. Math. Biol.* 38 (1999) 21–78.
- [9] B. Deng, Food chain chaos due to junction-fold point, *Chaos* 11 (2001) 514–525.
- [10] B. Deng, G. Hines, Food chain chaos due to Shilnikov orbit, *Chaos* 12 (2002) 533–538.
- [11] B. Deng, G. Hines, Food chain chaos due to transcritical point, *Chaos* 13 (2003) 578–585.
- [12] B. Deng, Food chain chaos with canard explosion, *Chaos* 14 (2004) 1083–1092.
- [13] B. Deng, Equilibrizing all food chain chaos through reproductive efficiency, *Chaos* 16 (2006) 043125, doi:10.1063/1.2405711 (7 p.).
- [14] B. Deng, I. Loladze, Competitive coexistence in stoichiometric chaos, *Chaos* 17 (2007) 033108, doi:10.1063/1.2752491 (14 p.).
- [15] B. Deng, Conceptual and circuit models of neurons, *J. Integrative Neurosci.* 8 (2009) 255–297.
- [16] B. Deng, Metastability and plasticity in some conceptual models of neurons, *J. Integrative Neurosci.* 9 (2010) 31–47.
- [17] B. Deng, Optimizing a communication system by neural circuits: The magic number 4 and golden ratio, 2007.
- [18] B. Deng, Decimal spike code maximizes neural memory against retrieval time, preprint, 2007.
- [19] B. Deng, Neural spike renormalization. Part II – Multiversal chaos, *J. Differential Equations* (2010), doi:10.1016/j.jde.2010.10.004, in press.
- [20] M. Feigenbaum, Quantitative universality for a class of nonlinear transformations, *J. Stat. Phys.* 19 (1979) 25–52.
- [21] M. Feigenbaum, The universal metric properties of nonlinear transformation, *J. Stat. Phys.* 21 (1979) 669–709.
- [22] O.E. Lanford III, A computer-assisted proof of the Feigenbaum conjectures, *Bull. Amer. Math. Soc.* 6 (1982) 427–434.
- [23] J. Palis, W. De Melo, *A geometrical introduction to dynamical systems*, Springer-Verlag, 1982.